SUPPLEMENTARY INFORMATION

Structural Basis for the Activation of Proteinase-Activated Receptors PAR1 and PAR2

Zongyang Lyu[1*], Xiaoxuan Lyu[1*], Andrey G. Malyutin[1*], Guliang Xia[1], Daniel Carney[1], Vinicius M. Alves[1], Matthew Falk[1], Nidhi Arora[1], Hua Zou[1], Aaron P. McGrath[1✉], Yanyong Kang[1✉]

[1] Takeda Development Center Americas, Inc, 9625 Towne Centre Drive, San Diego, CA 92121, USA

[*] These authors contributed equally: Zongyang Lyu, Xiaoxuan Lyu, Andrey Malyutin

✉email: aaron.mcgrath@takeda.com, kangyanyong@gmail.com

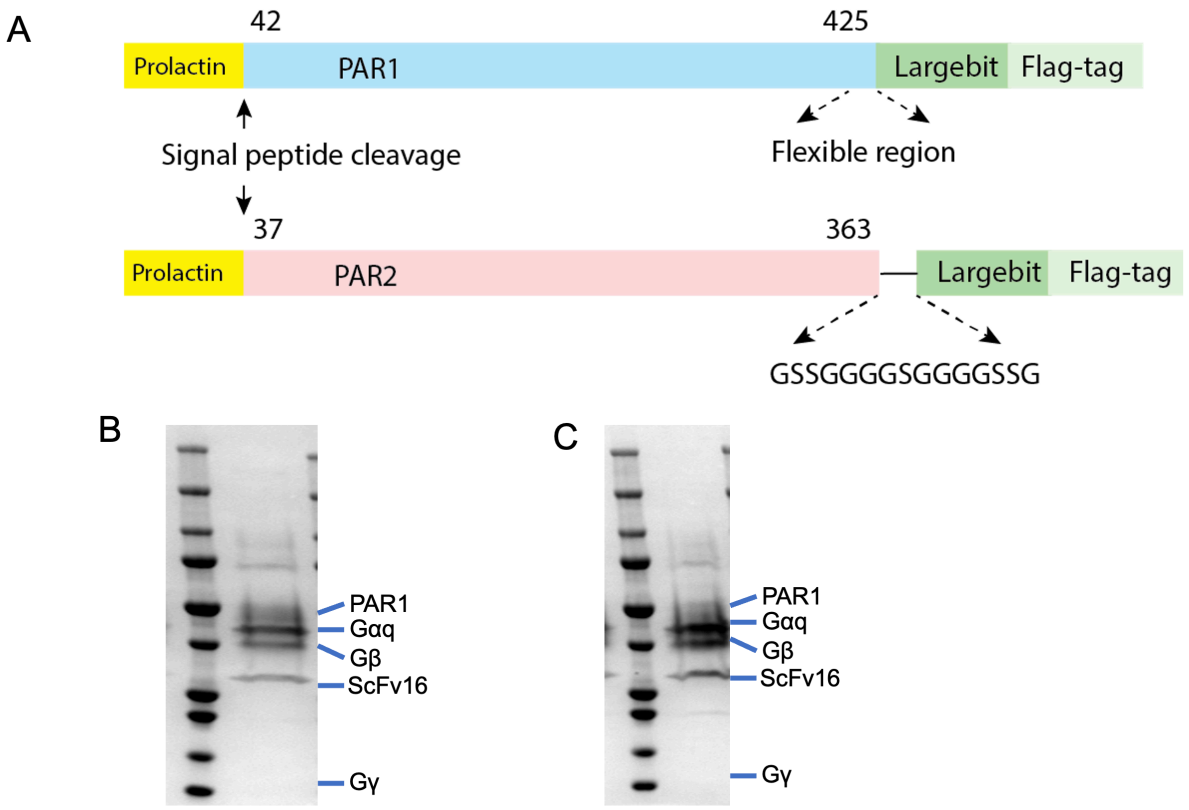

Supplementary Figure 1. **Construct design and protein purification**
A. Schematic representation of human PAR1 and PAR2 constructs. **B.** SDS-PAGE analysis of protein sample used for cryo-EM structural determination of PAR1-Gαq-scFv complex and **C.** PAR1-Gαq-scFv complex.

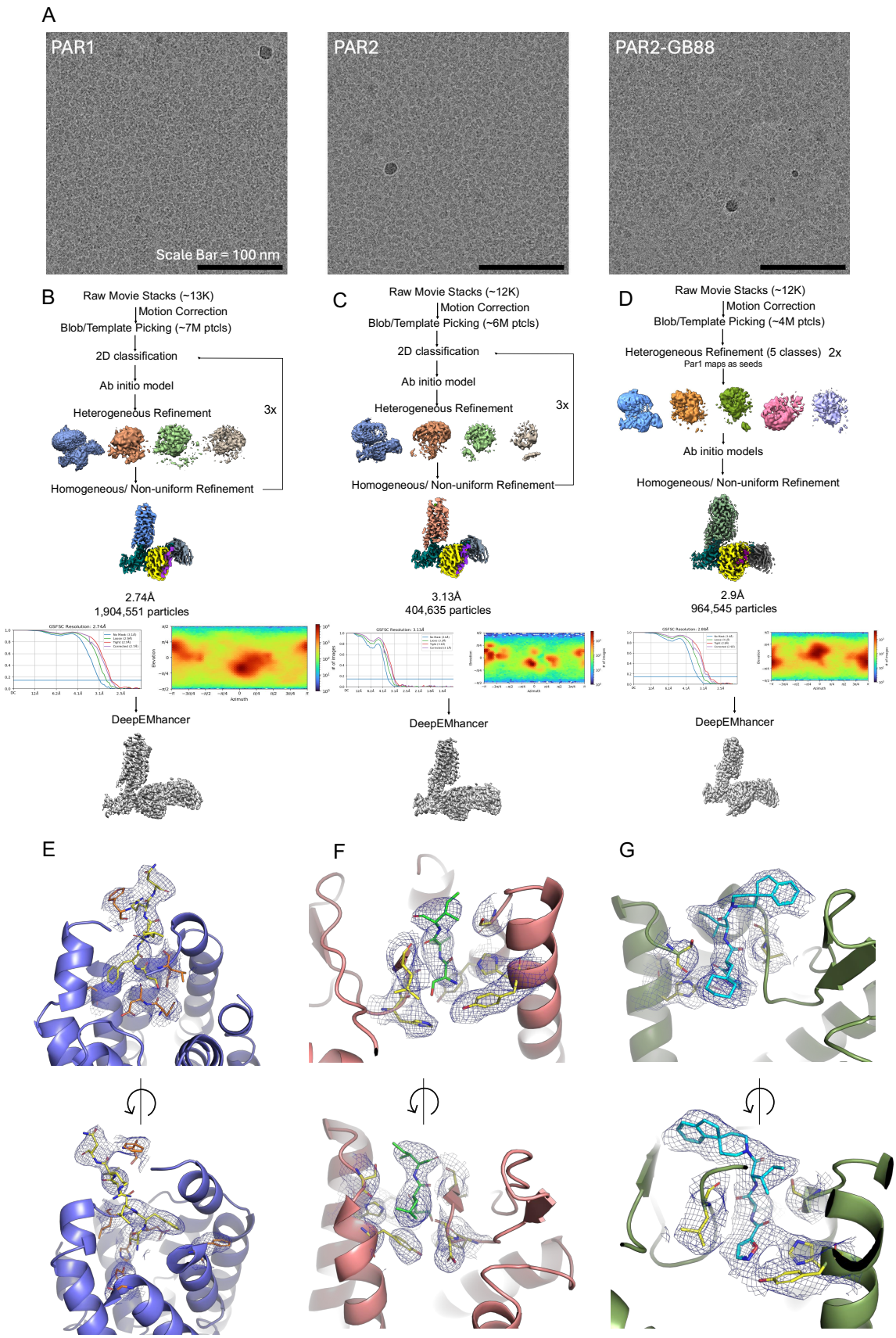
A
PAR1
Scale Bar = 100 nm
PAR2
PAR2-GB88
B
Raw Movie Stacks (~13K)
Motion Correction
Blob/Template Picking (~7M ptcls)
2D classification
Ab initio model
Heterogeneous Refinement
3x
Homogeneous/ Non-uniform Refinement
2.74Å
1,904,551 particles
DeepEMhancer
C
Raw Movie Stacks (~12K)
Motion Correction
Blob/Template Picking (~6M ptcls)
2D classification
Ab initio model
Heterogeneous Refinement
3x
Homogeneous/ Non-uniform Refinement
3.13Å
404,635 particles
DeepEMhancer
D
Raw Movie Stacks (~12K)
Motion Correction
Blob/Template Picking (~4M ptcls)
Heterogeneous Refinement (5 classes) 2x
Par1 maps as seeds
Ab initio models
Homogeneous/ Non-uniform Refinement
2.9Å
964,545 particles
DeepEMhancer
E
F
G

Supplementary Figure 2. Cryo-EM analysis of PAR1-Gαq, PAR2-Gαq, and PAR2-GB88 complexes.
A. Representative cryo-EM micrographs for PAR1-Gαq, PAR2-Gαq, and PAR2-GB88. **B.** Cryo-EM single-particle image processing workflow for PAR1-Gαq, **C**. PAR1-Gαq complex, and **D.** PAR2-GB88 complex. **E-G.** Visualization of PAR1 tethered ligand, PAR2 tethered ligand, and GB88, along with their interacting residues shown superimposed on a cryo-EM map (5 sigma) at two angles, spaced 180° apart.

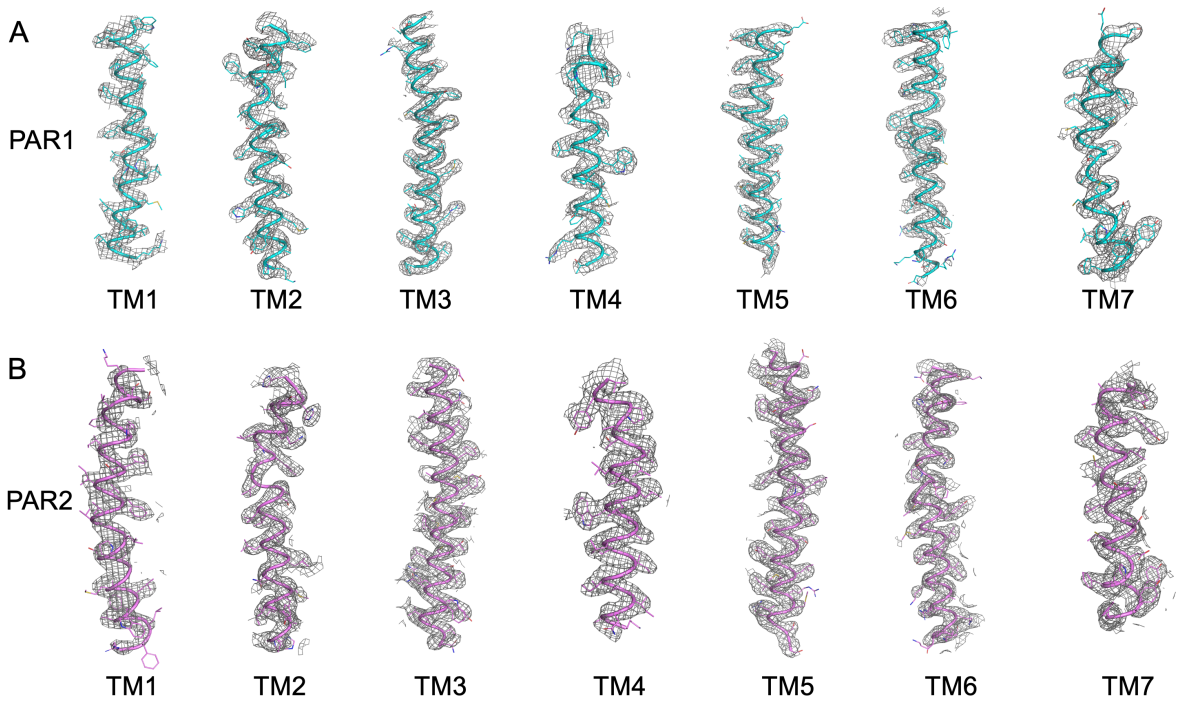

Supplementary Figure 3. Density maps of PAR1-Gαq and PAR2-Gαq complexes
A. Depicts the representative map of TM1-TM7 of PAR1 within PAR1-Gαq complex. **B**. Depicts the representative map of TM1-TM7 of PAR2 within PAR1-Gαq complex. Maps are shown at 5 sigma.

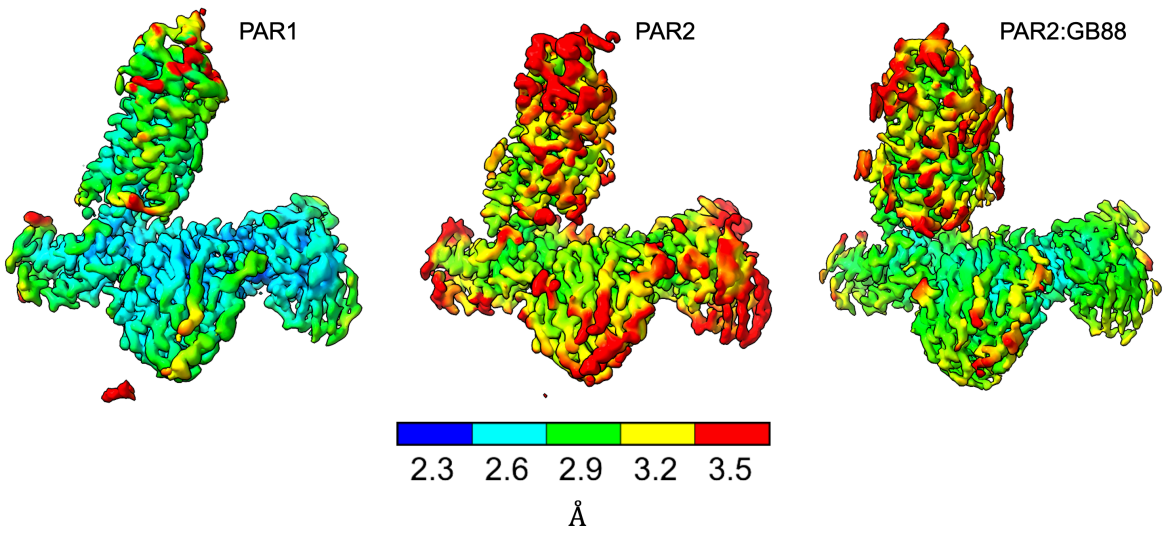

Supplementary Figure 4. Local resolution maps
Local resolution estimates for cryo-EM maps described in this study. Local resolution is illustrated by variation in map surface color and was estimated using cryoSPARC.

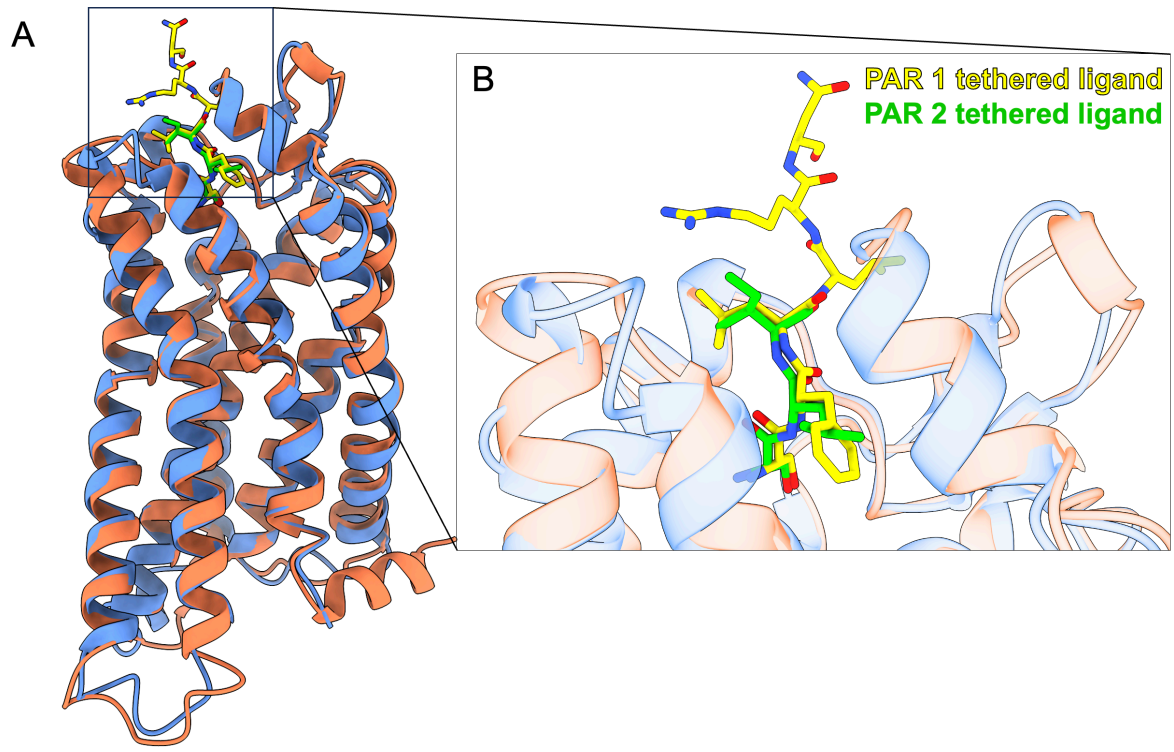

Supplementary Figure 5. Comparison of PAR1 and PAR2 with their tethered ligands
A. Structural superposition of the PAR1(blue) and PAR2 (orange). **B**. Position of the PAR1 tethered peptide (yellow) and the tethered peptide of PAR2 (green).

Supplementary Table 1. Cryo-EM data collection, refinement and validation statistics.

	PAR1-Gαq (PDB: 9D4Z)	**PAR2-Gαq (PDB: 9D0A)**	**PAR2-GB88 (PDB: 9E7R)**
Data collection and processing			
Magnification	165K	165K	165K
Voltage (kV)	200	200	200
Electron exposure ($e^-/Å^2$)	45	45	45
Defocus range (μm)	-0.8 to -2.0	-0.8 to -2.0	-0.8 to -2.0
Pixel size (Å)	0.69	0.69	0.69
Symmetry imposed	C1	C1	C1
Initial particle images (no.)	7,045,823	6,134,573	4,008,362
Final particle images (no.)	1,904,551	404,635	964,545
Map resolution (Å)			
FSC threshold	0.143	0.143	0.143
Map resolution (Å)	2.74	3.1	2.9
Refinement			
Model resolution (Å)	2.7	3.1	2.9
FSC threshold	0.5	0.5	0.5
Model-Map CC (mask)	0.73	0.73	0.73
Model composition			
Non-hydrogen atoms	8267	8416	8108
Protein residues	1067	1083	1043
B factors ($Å^2$)			
Protein	69.00	78.28	71.25
R.m.s. deviations			
Bond lengths (Å)	0.004	0.004	0.004
Bond angles (Å)	0.585	0.971	0.968
Validation			
MolProbity score	1.59	1.72	1.49
Clash score	6.12	7.74	4.83
Rotamer outliers (%)	0.00	0.00	0.83
Ramachandran plot			
Favored (%)	96.28	95.67	96.38
Allowed (%)	3.72	4.33	3.62
Outlier (%)	0	0.00	0.00